Multiwavelets applied to metal–ligand interactions: Energies free from basis set errors

Cite as: J. Chem. Phys. **154**, 214302 (2021); https://doi.org/10.1063/5.0046023
Submitted: 31 January 2021 • Accepted: 02 May 2021 • Published Online: 02 June 2021

Anders Brakestad, Peter Wind, Stig Rune Jensen, et al.

The Journal of Chemical Physics ARTICLE scitation.org/journal/jcp

Multiwavelets applied to metal–ligand interactions: Energies free from basis set errors

Cite as: J. Chem. Phys. 154, 214302 (2021); doi: 10.1063/5.0046023
Submitted: 31 January 2021 • Accepted: 2 May 2021 •
Published Online: 2 June 2021

Anders Brakestad,[1,2] Peter Wind,[1,2] Stig Rune Jensen,[1,2] Luca Frediani,[1,2,a)] and Kathrin Helen Hopmann[2,a)]

AFFILIATIONS

[1] Hylleraas Centre for Quantum Molecular Sciences, UiT The Arctic University of Norway, 9037 Tromsø, Norway
[2] Department of Chemistry, UiT The Arctic University of Norway, 9037 Tromsø, Norway

Note: This paper is part of the JCP Special Collection in Honor of Women in Chemical Physics and Physical Chemistry.
[a)]**Authors to whom correspondence should be addressed:** luca.frediani@uit.no and kathrin.hopmann@uit.no

ABSTRACT

Transition metal-catalyzed reactions invariably include steps where ligands associate or dissociate. In order to obtain reliable energies for such reactions, sufficiently large basis sets need to be employed. In this paper, we have used high-precision multiwavelet calculations to compute the metal–ligand association energies for 27 transition metal complexes with common ligands, such as H_2, CO, olefins, and solvent molecules. By comparing our multiwavelet results to a variety of frequently used Gaussian-type basis sets, we show that counterpoise corrections, which are widely employed to correct for basis set superposition errors, often lead to underbinding. Additionally, counterpoise corrections are difficult to employ when the association step also involves a chemical transformation. Multiwavelets, which can be conveniently applied to all types of reactions, provide a promising alternative for computing electronic interaction energies free from any basis set errors.

I. INTRODUCTION

A large branch of computational chemistry deals with the study of reaction mechanisms.[1,2] Many of the studied reactions involve metal complexes that throughout the course of the reaction bind or lose a ligand, for example, there may be incoming substrates such as alkenes or hydrogen (H_2) or leaving ligands such as solvent or product molecules (Scheme 1).[3–10]

The difficulty of contemporary density functional theory (DFT) methods to accurately compute metal–ligand interactions has been highlighted in the literature.[11–22] Many of the reported studies focus on the performance of different DFT functionals and the importance of including dispersion corrections in the computed energies.[11,15] There is less focus on the importance of choosing an adequate basis set.[23–25]

The most widely employed basis sets in computational chemistry are based on Gaussian-type orbitals (GTOs). Popular choices for computing reaction energies include, for example, the Pople split-valence or the Ahlrichs def2 basis sets.[26,27] Such bases may come in different sizes, with many contemporary DFT studies on metal-systems reporting final energies that were computed using double-ζ (DZ) or medium-sized triple-ζ (TZ) Pople basis sets[28–36] or the somewhat larger triple-ζ Ahlrichs basis set def2-TZVP.[37–40] The use of the correlation-consistent Dunning basis sets appears less widespread for transition metal systems.[41] Regardless of size, all available basis sets are finite, and therefore, they invariably carry a certain *Basis Set Error* (BSE), defined as the difference in energy (E) between the complete basis set (CBS) result and the finite basis set (FBS) result,

$$\mathrm{BSE} = E_{\mathrm{FBS}} - E_{\mathrm{CBS}}. \tag{1}$$

A complete basis set is infinite and therefore a certain level of truncation in the molecular orbital expansion must be accepted for any basis set. This fact is referred to as the "basis set truncation problem" and puts very concrete limitations on quantum chemical calculations. It is, in addition, not possible to know the extent of the BSE for a given basis set although the variational principle guarantees that enlarging a basis will reduce the BSE. In practical applications of GTOs, users often rely on a favorable cancellation of BSEs, where large errors in absolute energies are partly canceled, when relative energies (e.g., the energy difference between two states) are computed.

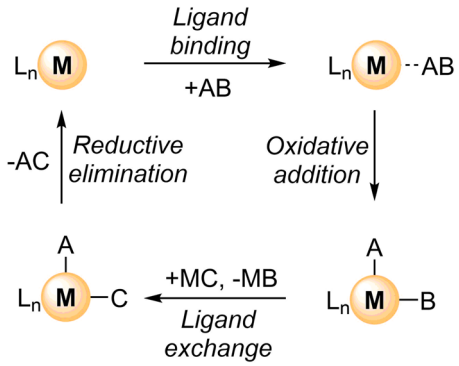

SCHEME 1. Generic example of a metal-catalyzed reaction pathway (e.g., a cross-coupling reaction, M = metal) where ligands enter and leave.

In the case of a geometrical rearrangement and, in particular, when considering association or dissociation reactions, the BSE can be divided into two different (though not completely independent) types of errors: the Basis Set Superposition Error (BSSE) and the remaining Basis Set Incompleteness Error (BSIE).[23,25,42] The BSSE originates from the fact that atom-centered basis functions follow the nuclear positions. Therefore, the molecular orbitals will be represented by different basis sets when comparing two different geometries because the basis functions will overlap differently (or in some cases not at all) before and after the geometrical change.[43–45] The BSIE can then be considered as the remaining error with respect to the CBS result, although it is important to underline that the two errors cannot be separated completely, and both will approach zero in the limit of a CBS.

The most notable example where the BSSE becomes prominent is when two molecules are joined into one model, as illustrated in Fig. 1. In this case, the "borrowing of basis functions" effectively improves the basis set description of the combined molecules compared to the separated molecules, which can lead to an artificial lowering of the energy.

A common strategy for dealing with the BSSE is to use the Boys and Bernardi counterpoise (CP) correction.[43] The CP correction is often applied for association reactions of non-covalently interacting fragments,[25,46,47] but it is also employed when computing metal–ligand interactions, for example, as part of a reaction cycle.[14,48,49] The theoretical justification for the CP correction has been the subject of much scientific debate since its introduction.[44,50,51] A mathematical proof was published in 1994, which demonstrated that the CP correction eliminates intermolecular BSSEs in simple complexation reactions for full CI (FCI) wave functions.[44] However, similar theoretical arguments have, to our knowledge, not been presented for DFT.

The CP correction is typically computed on the basis of the complexed system, which is partitioned into fragments, whose energies are computed in the presence and absence of the basis functions of other fragments. For non-covalent association and dissociation reactions, the partitioning is simple, but for reactions where the combination of fragments involves bond-breaking, the partitioning becomes ambiguous. As an example, let us consider two reactions: one where CO_2 binds to a complex (Scheme 2, left) and one where CO_2 is inserted into a metal–ligand bond (Scheme 2, right). For the simple association reaction, the original fragments remain and partitioning is straightforward, but for the insertion reaction, the original fragments no longer exist in the product and it is thus unclear how the system should be partitioned. Reaction types other than simple associations and dissociations are widespread in transition metal-mediated chemistry, such as oxidative additions, reductive eliminations, insertions, transmetallations, and metathesis pathways—for all of these, it is not straightforward how to apply a CP protocol.

Another approach for reducing BSEs is to employ a large basis set. It is a relatively standard procedure in computational studies to perform single-point electronic energy calculations with a larger basis set using optimized geometries computed with a smaller basis set. The large basis sets used for energy calculations may still not be sufficient (as pointed out by Head-Gordon and co-workers, it is remarkably difficult to reach the basis set limit, requiring very large basis sets, such as the quintuple-ζ basis set pc-4);[47] however, for practical applications on first- and second-row elements, and also smaller 3d complexes, basis sets up to the quadruple-ζ-level can routinely be applied and provide good results.[47,52] The situation is different for larger metal-based systems, where quadruple-ζ basis sets may not be available, may be too costly, or may cause numerical instabilities, implying that for metal systems, single-point corrections often are carried out with triple-ζ basis sets, sometimes in combination with an effective core potential on the metal. However, triple-ζ basis sets from different basis set families may perform very differently, and for some of the widely applied basis

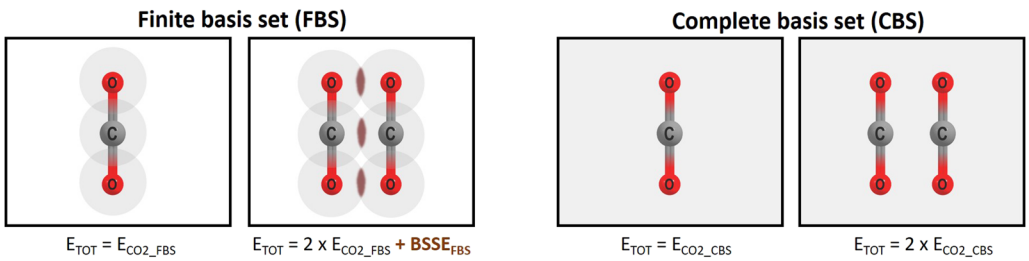

FIG. 1. (Left) When two molecules or fragments are joined into one computational model, the fragments can steal basis functions from each other, artificially lowering the total energy (E_{tot}) of the combined model (an error known as the BSSE). (Right) In a complete basis set, the stealing of basis functions does not occur (the shown systems are only illustrations and do not correspond to optimized models).

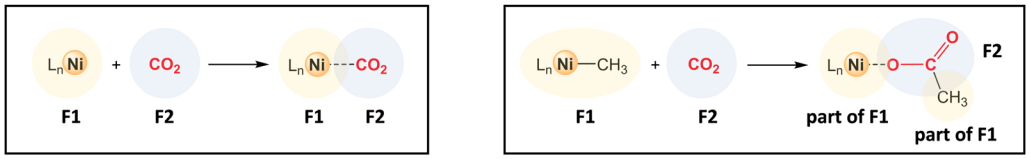

SCHEME 2. (Left) Simple association reaction, where the complex formed after association easily can be partitioned into the original fragments F1 and F2 in order to compute the BSSE. (Right) Association reaction involving a chemical transformation, where the partitioning into original fragments becomes ambiguous, and it is unclear how the BSSE should be computed.

sets, such as 6-311G(d,p),[31–34,36] the BSE may still be significant (*vide infra*).

In recent years, a new strategy, based on real space methods,[53] has emerged, which can resolve BSE issues in a fundamental and uncontroversial way. In contrast to atom-centered functions, real space methods represent functions as values on a grid. As the representation is fixed in space and does not follow the molecule, the source of BSSE is eliminated. In this respect, the methods based on Multiresolution Analysis (MRA)[54–56] and Multiwavelets (MWs)[57–59] are particularly attractive: molecular orbitals are represented using polynomials on a predefined grid. Such a grid can be arbitrarily refined by bisection to gain precision, and the refinement is adaptive: it is based on the wavelet norm of a function at a given node, which guarantees rigorous error bounds based on MRA.[60] This means, in practice, that refinement takes place only where necessary (typically close to the nuclei), thus reducing the computational overhead with respect to full-grid methods. Other cornerstones of this approach are the use of the integral formulation for the Kohn–Sham equations,[57,61] which allows the use of integral operators instead of differential ones, the separated representation of Green's function kernels,[62] which reduces the computational overhead, and the non-standard form of operators,[60] which enables adaptivity also when operators are applied.

This robust mathematical framework of MWs simplifies the computational protocol substantially compared to GTO calculations: The vast choice of GTO basis sets require expert knowledge to fine-tune the basis to the problem at hand; hence, many practitioners fall back to familiar but suboptimal options such as standard double- or triple-ζ basis sets. MWs, on the other hand, deal with the mathematical complexity in a robust and formally rigorous way, exposing to the user only a few parameters to set the requested precision. This offers a simple protocol, both practically and intellectually, for obtaining energies that are free from basis set errors to within an arbitrary and predefined threshold. We have recently employed MW methods to obtain precise benchmarks on energies[63] and electric[64] and magnetic properties.[65]

In this work, we have used multiwavelets to compute the electronic energies for 27 transition metal-mediated reactions, which involve association of common ligands such as H_2, CO, olefins, or solvent molecules. To our knowledge, MWs have not been previously used to compute transition metal systems, although it has been suggested that by using them, one could improve the results for DFT calculations involving metals.[66] Comparing our multiwavelet interaction energies to the results obtained with a variety of GTO-type DZ, TZ, and QZ basis sets, we show that BSEs in commonly used GTO basis sets can be very large. Interestingly, the use of the counterpoise correction to correct for BSSEs may lead to significant underbinding for metal–ligand interactions, potentially bringing the corrected value as far from the MW reference value as the uncorrected one.

II. COMPUTATIONAL DETAILS

A. Choice of reactions

The set of association reactions was based on the following criteria: (1) The reactions should be simple association reactions so that standard counterpoise corrections could be applied, (2) the complexes should feature 3d transition metals in order to limit the system size, also because not every all-electron basis set studied here is available for heavier metals, (3) the incoming ligands should be experimentally relevant and of varying sizes, (4) the nature of the metal–ligand binding should be diverse, and (5) all chemical species should have a closed-shell electronic configuration.

Our benchmark reaction set includes 26 transition metal-mediated association reactions, with the full list presented in Schemes 3(a)–3(c). Four of these reactions, namely, Cr–CO, Cr–H_2, Cr–alkene-1, and Ni–CO, were chosen from Ref. 19 (but we note that some of these reactions have been studied computationally much earlier[67]), and one, Fe–MeOH, is related to our previous work on Fe-catalyzed hydrogenation reactions.[68] Based on the Cr and Ni examples, we designed additional reactions involving association of differently sized alkenes (alkene-1–alkene-6), different solvent molecules (MeCN, THF, MeOH, and H_2O), and common NHC ligands (NHC-1 and NHC-2, Scheme 3). The optimized coordinates of all species are given in the supplementary material.

One additional CO_2 insertion reaction was computed [Scheme 3(d)] as an example of a reaction, where CP corrections become ambiguous to compute, as the original fragments are no longer present in the product. This reaction is not included in the benchmark averaging, but it is discussed separately.

B. GTO calculations

All GTO calculations were performed with ORCA[69,70] versions 4.1.2 and 4.2.1 (see supplementary material, Table S1 for further details) within the restricted Kohn–Sham DFT framework.[71,72] The SCF cycles were accelerated by the RI[73–79] and RI-COSX[115] approximations for GGA and hybrid functionals, respectively. A multigrid scheme was used for the integration grids: Intermediate SCF iterations made use of an angular Lebedev grid of 434 points and a radial grid of 30, 35, and 40 points for first, second, and third row elements, respectively (as defined by the *grid*5 ORCA keyword). A final

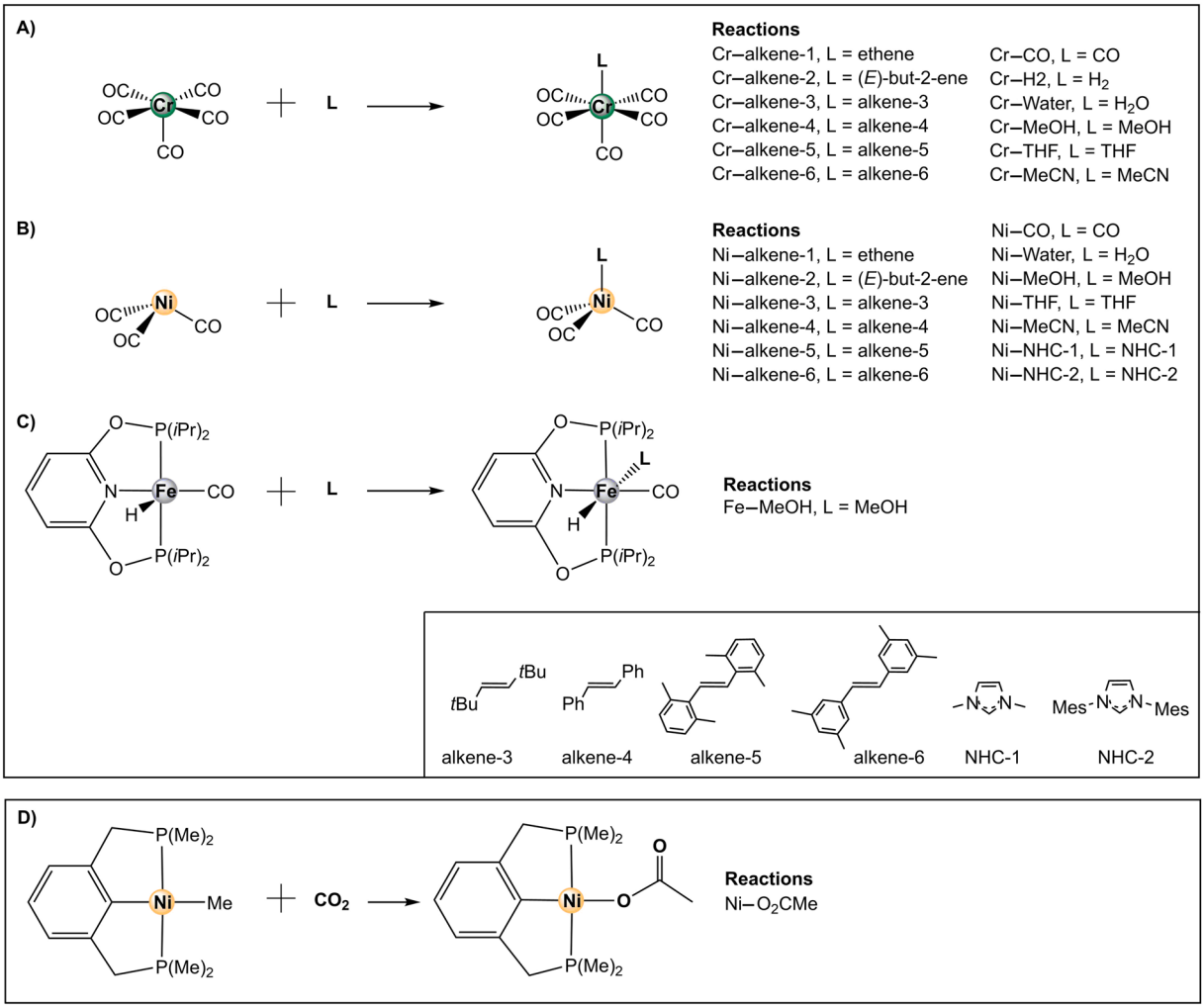

SCHEME 3. Overview of the 26 association reactions included in our dataset (a)–(c) as well as one CO_2 insertion reaction discussed separately (d).

SCF computation was then carried out with a larger angular Lebedev grid of 590 points and a radial grid of 40, 45, and 50 points for first, second, and third row elements, respectively (as defined by the *finalgrid*6 ORCA keyword).

All geometries were optimized in vacuum with the def2-SVP basis set[27] and included Grimme's third generation dispersion correction with Becke–Johnson damping functions.[80,81] For the data presented in the main text, we used the PBE functional;[82–84] however, in the supplementary material, we also present results with BP86 and PBE0.[85,86] The BP86 and PBE0 results are in close qualitative agreement with PBE (supplementary material, Figs. S1–S12). Default SCF convergence thresholds were used for the geometry optimizations. Geometry convergence criteria were set by the *tightopt* ORCA keyword, which sets convergence thresholds for the energy change, maximum gradient, rms gradient, maximum structural displacement, and rms structural displacement as 1×10^{-6}, 1×10^{-4}, 1×10^{-5}, 1×10^{-3}, and 1×10^{-4}, respectively (in atomic units). Finally, a frequency analysis was performed in order to confirm that the optimized structures represented minima on the potential energy surface.

Single-points and counterpoise corrections were performed with ORCA versions 4.1.2 and 4.2.1. SCF convergence was dictated by the *tightscf* ORCA keywords, which signals convergence if the changes in the total energy and one-electron energy fall below 1×10^{-8} and 1×10^{-5}, respectively. A range of commonly used GTO basis sets of different sizes were employed in this benchmark study, with examples from Jensen's polarization-consistent basis sets,[87–90] Ahlrichs' property-optimized def2 basis sets,[27] Dunning's correlation-consistent basis sets,[91–94] Pople's split-valence basis sets,[26,95–102] and a popular combination of Pople basis sets with the LANL2 ECP and accompanying valence basis set.[103]

The GTO basis sets included in this study are as follows:

- Ahlrichs: def2-QZVPPD, def2-QZVPP, def2-TZVPD, def2-TZVP, def2-SVPD, and def2-SVP;

- Dunning: aug-cc-pVQZ, cc-pVQZ, aug-cc-pVTZ, cc-pVTZ, aug-cc-pVDZ, and cc-pVDZ;
- Pople: 6-311++G(2df,2pd), 6-311+G(d,p), 6-311G(d,p), 6-31+G(d), and 6-31G(d) (with additional 6-311G and 6-31G results given in supplementary material, Figs. S1–S4);
- 6-311G(d,p) (nonmetals)/LANL2TZ (metals); and
- Jensen: pc-3, aug-pc-2, pc-2, aug-pc-1, and pc-1 (with additional aug-pc-3 results given in supplementary material, Figs. S1–S4 and S18).

C. Linear dependencies in large GTO basis sets

Numerical issues can become a problem for larger GTO basis sets. The overlap between functions centered on different atoms may become significant, especially for larger molecules, such that near-linear dependencies occur. GTO codes such as ORCA evaluate the presence of linear dependencies by diagonalizing the overlap matrix and discarding eigenvalues and corresponding basis functions below a certain threshold (10^{-8} is the default for ORCA). For the association reactions studied here (Scheme 3), near-linear dependencies occurred more frequently for the adduct than the separated fragments. In most cases where the default threshold was employed, only a handful of functions were discarded (supplementary material, Table S3), which should have no significant effect on the energies, because such near-linearly dependent functions by definition are close to being redundant. Most near-linear dependencies were observed for the basis sets aug-pc-2 and aug-pc-3, where the SCF iteration converged only if a larger threshold (up to 10^{-4}) was employed (supplementary material, Tables S3 and S4). In several instances, this resulted in several hundred functions being discarded for aug-pc-3 (more than 10%–15% of the functions). Consequently, we have not discussed the aug-pc-3 results in the main text, but only in the supplementary material (Fig. S18), in order to show the effect from computing interaction energies from individual SCF calculations performed with different linear dependency thresholds. Thus, the seemingly lower precision achieved by aug-pc-3 compared to pc-3 (supplementary material, Fig. S18) is not due to inherent basis set deficiencies but due to a sub-optimal computational protocol necessary for converging the SCF calculations.

D. Multiwavelet calculations

All MW calculations were carried out with the free and open-source MRChem quantum chemical software, release version 1.[104] Information about how to obtain, compile, and use the code is available on the documentation web pages.[105] A computational domain with the size (−64, 64) in all three dimensions (angstroms) was used for all molecular systems, with the molecular structure translated such that the center-of-mass was in the origin of the computational domain. A relative precision of 1×10^{-7} a.u. (MW7) was used in the generation of our MW data. Two convergence criteria were applied in the SCF optimizations: The change in total energy should be below 1×10^{-7} a.u., and the orbital residuals should be at least 5×10^{-6}. We remark that the electronic energy is variationally optimized and its error is therefore quadratic in the orbital error. The error threshold of the orbitals should be set to $\sqrt{\varepsilon_{rel}}$ in order to guarantee that the total energy has been converged to ε_{rel}. By setting the orbital residual convergence threshold to $50\varepsilon_{rel}$, we made a conservative choice in converging the orbital residuals. The SCF procedure was accelerated by the Krylov accelerated inexact Newton procedure.[106]

E. Internal validation of MW convergence

Multiwavelet energies represent the CBS limit within the specified precision. When MWs are employed to compute reaction energies, it is important to bear in mind that error cancellation does not take place when one energy is subtracted from another; instead, one relies on numerical robustness. As a result, care must be taken when two energies (e.g., reactants and products) are subtracted: one must ensure that the number of significant digits is large enough to guarantee that enough precision is retained in the difference. However, for MWs, this is a systematic and controllable procedure, as opposed to relying on error cancellation in GTO protocols, whose extent is not known *a priori* and which cannot be controlled.

In order to obtain a sufficient number of significant digits in the interaction energy, an appropriate MW precision needs to be used in calculations of individual energies. We evaluated increasing MW precisions for a subset of the reactions in order to determine the appropriate precision for our dataset (Table I). A low precision of 1×10^{-4} (MW4) contains a lot of noise because of cancellation of significant digits. However, increasing the precision to 1×10^{-6} (MW6) yields a precision of minimum 0.1 kcal/mol, with an even higher precision observed for most reactions. For the benchmark data in the main text, we made a conservative choice and used the MW7 interaction energies in our analyses, which our data show to be correct to ~1 cal/mol for the cases, where we can compare to MW8 data.

Note that the MW validation data presented in Table I was computed with BP86, while the benchmark data discussed in the main text was computed with PBE. This discrepancy is due to an unforeseen challenge that arose during data collection: originally all MW and GTO data were computed with BP86, but we later realized that the BP86 versions in ORCA and MRChem are not identical, implying that a comparison of GTO to MW at the BP86 level would be affected by differences in the implementation of the functional, which our tests indicated could amount to several kcal/mol, when approaching the CBS limit. Therefore, the GTO to MW comparison in the main text was based on the PBE functional. We also present a smaller MW validation analysis with the PBE functional in the supplementary material with 1×10^{-5} (MW5) and 1×10^{-7} (MW7) precisions. The average error of the 1×10^{-5} energies compared to the 1×10^{-7} reference is 0.0635 kcal/mol, which is close to the error observed with the BP86 functional in Table I for the same precision.

III. RESULTS AND DISCUSSION

Initially, we present an analysis of the magnitude of the BSSE with various DZ, TZ, and QZ GTO basis sets for 26 transition metal-mediated association reactions (Scheme 3). This is followed by an analysis of the effect of the counterpoise correction—does it bring the GTO results closer to the MW-computed CBS reference value? We then take a closer look at the 6-311G(d,p) basis set due to its unexpected poor performance. Finally, we show how MWs conveniently can be applied to compute CBS single point energies for insertion reactions.

TABLE I. Errors in electronic interaction energies (kcal/mol) computed with increasing MW precision. We computed all reactions with a precision of 1×10^{-4} (MW4), 1×10^{-5} (MW5), 1×10^{-6} (MW6), and 1×10^{-7} (MW7) and a few with 1×10^{-8} (MW8). The errors for MW4, MW5, and MW6 were obtained by comparing to MW7 results. The MW7 error was obtained relative to the few MW8 results. With MW6, one obtains at least one correct decimal in the interaction energy and mostly two or more decimals. With MW7, errors of less than 0.0002 kcal/mol are obtained, as shown by comparison to the MW8 results. n.a. = not available.

Reaction	Error MW4[a]	Error MW5[a]	Error MW6[a]	Error MW7[b]
Cr–alkene-1	0.907 79	0.024 00	0.001 06	0.000 07
Cr–alkene-2	1.805 26	0.035 88	0.002 13	−0.000 03
Cr–alkene-3	2.244 01	0.153 09	0.004 39	n.a.
Cr–alkene-4	0.214 15	0.056 98	0.005 08	n.a.
Cr–alkene-5	5.606 96	0.235 89	0.008 02	n.a.
Cr–alkene-6	2.078 54	0.157 67	0.012 48	n.a.
Cr–water	1.780 81	0.041 22	0.000 97	n.a.
Cr–MeOH	1.152 02	0.010 78	−0.000 47	n.a.
Cr–THF	2.440 00	0.097 63	0.003 32	n.a.
Cr–MeCN	1.113 60	0.074 43	0.000 89	n.a.
Cr–CO	4.100 96	0.080 51	0.003 71	n.a.
Cr–H2	1.001 21	0.041 25	0.00 209	n.a.
Ni–alkene-1	−1.132 59	−0.014 61	−0.000 86	0.000 12
Ni–alkene-2	1.692 24	0.061 70	0.002 08	0.000 04
Ni–alkene-3	−0.060 38	0.081 28	0.013 71	n.a.
Ni–alkene-4	1.503 49	0.140 09	0.002 95	0.000 02
Ni–alkene-5	2.676 60	0.127 06	0.006 44	n.a.
Ni–alkene-6	−0.911 28	0.061 07	0.002 72	n.a.
Ni–water	−1.117 14	−0.004 97	0.000 45	0.000 03
Ni–MeOH	−1.046 20	−0.013 19	−0.000 48	0.000 17
Ni–THF	1.142 78	0.045 61	0.002 91	n.a.
Ni–MeCN	−0.459 47	0.000 10	0.000 21	n.a.
Ni–CO	−0.003 76	0.015 38	−0.000 04	n.a.
Ni–NHC-1	0.665 76	0.067 70	0.003 49	n.a.
Ni–NHC-2	3.266 62	0.483 49	0.009 81	n.a.
Fe–MeOH	1.970 12	−0.136 80	−0.002 28	n.a.
Average	1.255 08	0.073 97	0.003 26	0.000 06

[a]Computed as ΔE [MWX] − ΔE [MW7], where X = 4, 5, and 6.
[b]Computed as ΔE [MW7] − ΔE [MW8].

A. How large are BSSEs for metal–ligand association reactions?

It has been reported that the magnitude of the BSSE relative to the non-covalent interaction energy for organic molecules starts off relatively small for minimal basis sets[107] and then increases as the size of the basis set increases, while it eventually diminishes to negligible magnitudes for very large GTO basis sets.[25] Medium-sized basis sets of DZ quality provided the largest BSSEs.

We have here computed 26 transition metal-mediated association reactions (Scheme 3) in order to get an overview of how large the BSSEs are in these kind of reactions with DZ, TZ, and QZ basis sets of different sizes and families. The reactions studied here involve ligands that bind to a metal complex, which are conceptually different from non-covalent interaction energies. We have built our test set to include ligands of various size, many of which are common incoming ligands in metal-catalyzed reactions (such as H_2, CO, alkenes, and methanol).[3–10]

Several features are observed from our computed results (Fig. 2, see also supplementary material, Figs. S1–S4). First, the magnitude of the BSSE is largest for DZ basis sets, with an average value of 9.92 kcal/mol for the 26 reactions with the basis set 6-31G(d,p). However, the BSSE is also unexpectedly large for the TZ basis set 6-311G(d,p), with 8.63 kcal/mol on average. The combination 6-311G(d,p) on non-metal atoms and LANL2TZ on the metal gives a significantly lower average BSSE value of 4.25 kcal/mol for the 26 reactions, but it is still much larger than the def2-TZVP basis set, with an average BSSE of only 1.05 kcal/mol (maximum value of 2.19 kcal/mol). By comparing all results, it becomes clear that the BSSEs decrease as the ζ-quality increases within each basis set family. However, comparing ζ-qualities between families does not necessarily follow the same trend. For example, the Jensen triple-ζ basis set pc-2 has an average BSSE of 0.69 kcal/mol, which is lower than the Dunning-type quadruple-ζ basis set cc-pVQZ (average error of 0.74 kcal/mol).

Zooming in on the computed reactions, we see that with almost all basis sets, the largest BSSEs are obtained for the Ni–NHC-2 reaction, which may seem unsurprising, as NHC-2 is the largest ligand in our test set. However, there is no clear correlation between

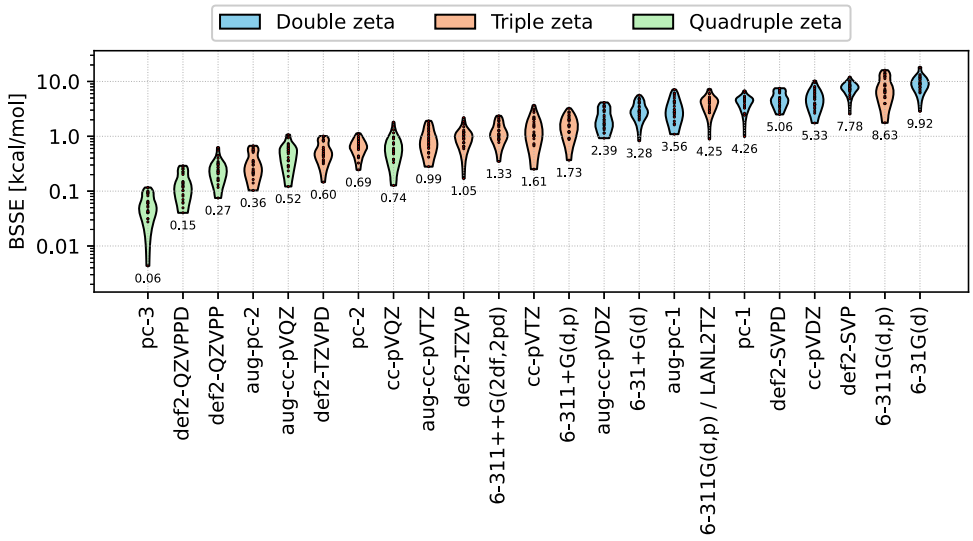

FIG. 2. Violin plot summarizing BSSEs (as computed by the counterpoise correction) for selected GTO basis sets (at the PBE level), sorted by ascending averages. The numbers show the average BSSE (kcal/mol) for all association reactions [Schemes 3(a)–3(c)] for a given basis set. Additional basis sets are given in supplementary material, Fig. S1.

the size of the incoming ligand and the BSSE. For example, even the association of a small ligand, such as CO, can give similar BSSEs as much larger ligands, as shown for different TZ basis sets in Fig. 3. For DZ and medium-sized TZ basis sets such as 6-311G(d,p), a clear correlation is observed for the type of metal, with BSSEs consistently being larger for the Ni complexes than for the corresponding Cr complexes (supplementary material, Fig. S3). This may be due to the fact that the $Cr(CO)_5$ scaffold is larger than the $Ni(CO)_3$ scaffold and therefore already has a more complete set of basis functions. For larger basis sets such as def2-TZVP, the BSSEs for the Cr and Ni systems with the same type of incoming ligand are more similar.

An important point of interest is how large the BSSE is *relative* to the interaction energy. BSSE proportions of (uncorrected) electronic interaction energies in our test set are presented in Fig. 4. For DZ, TZ, and QZ basis sets, the magnitudes of the BSSE are up to 60%, 50%, and 20% of the electronic interaction energy, respectively. An exception is 6-311G(d,p), for which the BSSE is about 100% of the interaction energy. Significant variance within each basis set is also observed, spanning at least one order of magnitude for most basis sets. Even interaction energies from large QZ basis sets contain significant proportions of BSSE of up to 20%.

B. Can CP corrections bring GTO energies closer to the CBS value?

We have computed the electronic interaction energies for the 26 reactions in our test set at the complete basis set limit by using a MW basis at high precision (1×10^{-7} = MW7, Table I). With these MW results as a reference, it is possible to gauge how close the uncorrected and CP-corrected GTO energies are to the CBS

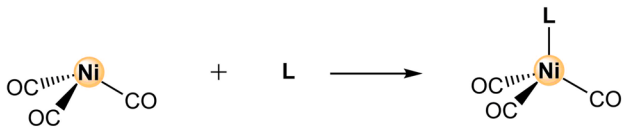

Reaction	L	6-311G(d,p)	6-311++G(2df,2dp)	def2-TZVP
Ni–CO	C=O	11.2	1.0	0.6
Ni–THF		9.0	1.0	0.9
Ni–NHC-2	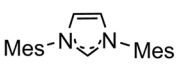	16.1	2.2	1.3

FIG. 3. BSSEs (kcal/mol) for three selected reactions with three TZ GTO basis sets (PBE level).

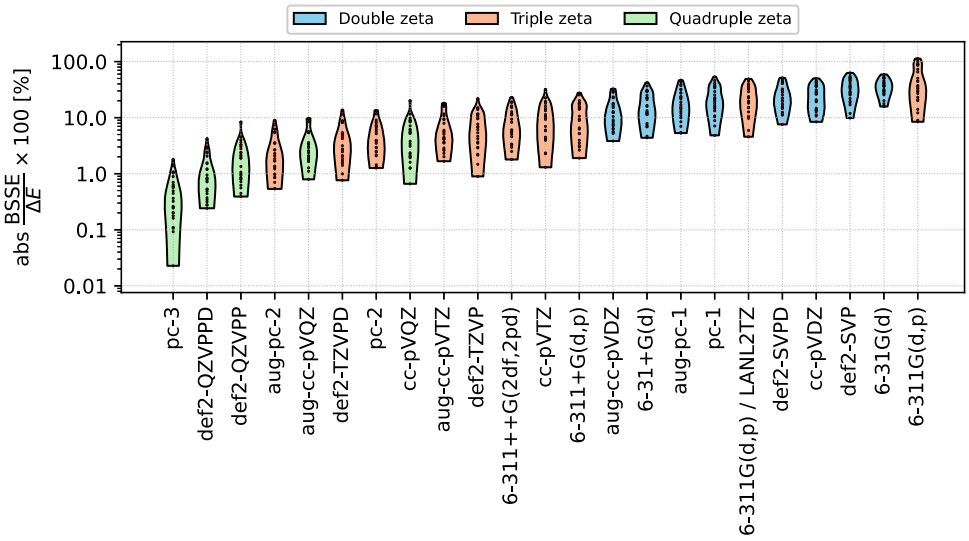

FIG. 4. Violin plot summarizing the proportion of electronic interaction energies due to the BSSEs, in percentages, sorted by ascending averages for selected basis sets (PBE level). Additional basis sets are given in supplementary material, Fig. S2.

limit. Table II shows the basis set errors (BSEs) at the triple-ζ level for the raw (CP-uncorrected) electronic interaction energies. The Pople basis sets perform worst, with even the largest augmented 6-311++G(2df,2pd) basis set showing an average absolute error of 1.4 kcal/mol. The augmented correlation-consistent Dunning basis set performs slightly better (average error of 1.0 kcal/mol), whereas the Ahlrichs and, especially, the Jensen basis sets perform very well, with errors below 0.8 kcal/mol and down to 0.3 kcal/mol for aug-pc-2 (Table II). The MW results thus provide a unique insight into the BSE of different basis set families at the DFT level.

Our MW analysis indicates that the signed BSEs are almost always negative (Table II), implying that the uncorrected basis sets overbind the complexes. What happens if a CP-correction is included to correct for the BSSE? In the top panel of Fig. 5, the GTO basis set errors are plotted on a linear y axis in order to show the different signs of CP-corrected and uncorrected interaction energies. It is evident that uncorrected interaction energies tend to approach the CBS limit from below (overbinding of the complex), while the CP-corrected interaction energies tend to approach from above (underbinding of the complex). This is in line with other work, indicating that including the full CP correction leads to underbinding.[108]

In the bottom panel of Fig. 5, the absolute value of the interaction energies is plotted on a logarithmic y axis in order to show the magnitudes of the errors for corrected and uncorrected interaction energies. Jensen's polarization-consistent basis sets perform the best within each ζ-quality, with the QZ basis set pc-3 delivering deviations from the CBS limit to within ~0.1 kcal/mol or less. The augmented version of pc-3 (aug-pc-3) is not reported here but discussed separately in the supplementary material due to the numerical issues encountered (Fig. S18). Figure 5 shows that the CP corrections tend to lower the average error for most basis sets, although there are notable exceptions, such as 6-311G(d,p) (Fig. 5) and 6-311G (supplementary material, Fig. S13). For these cases, the counterpoise correction does not make the absolute error in the electronic interaction smaller, as the CP-corrected value is as far from the reference value as the CP-uncorrected value, just with opposite sign. In order to illustrate how the BSSE and the counterpoise correction may affect the reaction energy of a specific reaction, consider reaction Ni–alkene-3 (Scheme 4), which has a medium-sized alkene as the incoming ligand (a typical substrate in metal-catalyzed reactions[109]) with a commonly used basis set, 6-311G(d,p).[31,33,112] The electronic association energy computed for this reaction is −14.0 kcal/mol with PBE/6-311G(d,p) (not including any other corrections). The computed BSSE at the same level is, however, 15.2 kcal/mol, resulting in an electronic association energy of +1.2 kcal/mol. The CP correction thus has a larger absolute value than the non-corrected electronic interaction energy. Typically, reported computational

TABLE II. Basis set errors (BSEs) for TZ basis sets (in kcal/mol) averaged over the CP-uncorrected electronic interaction energies for 26 association reactions.

TZ basis set	Average error[a]	Average absolute error[a]
6-311G	−4.7488	4.9925
6-311G(d,p)	−4.3721	4.3721
6-311G(d,p)/LANL2TZ	−3.1087	3.1287
6-311+G(d,p)	−1.9159	1.9159
6-311++G(2df,2pd)	−1.3753	1.3753
cc-pVTZ	−1.3930	1.3930
aug-cc-pVTZ	−1.0091	1.0091
def2-TZVP	−0.7756	0.7805
def2-TZVPD	−0.5085	0.5085
pc-2	−0.5127	0.5127
aug-pc-2	−0.3095	0.3162

[a]Average of basis set errors of GTO calculation for 26 reactions, each relative to the complete basis set limit computed with PBE as ΔE[GTO]−ΔE[MW7].

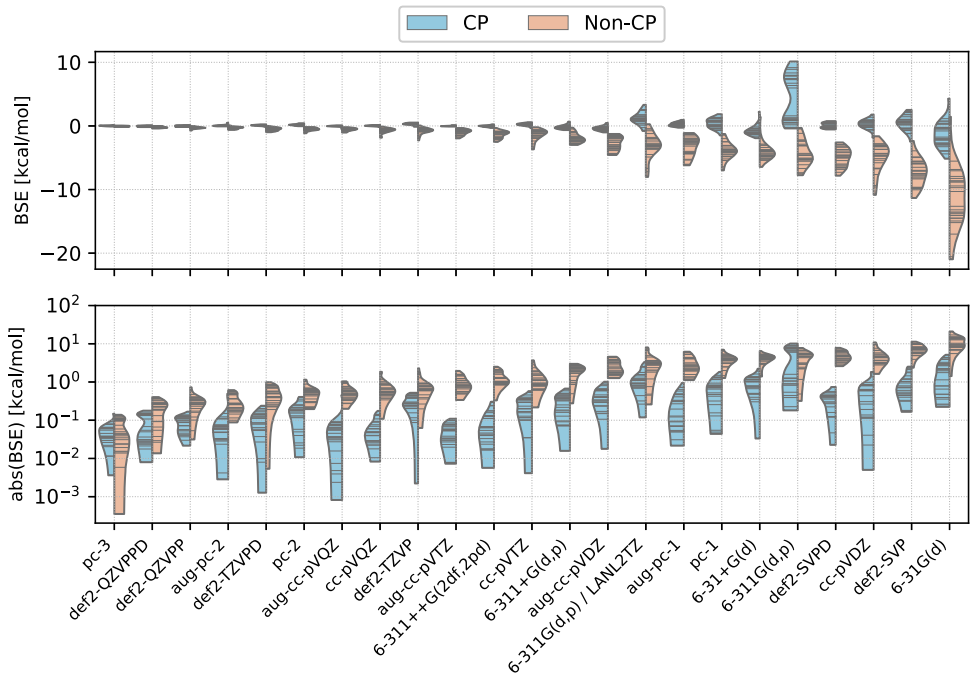

FIG. 5. Violin plot summarizing the basis set errors (in kcal/mol, PBE) for uncorrected and CP-corrected electronic interaction energies using our MW7 data as a reference. (Top) Basis set errors plotted on a linear axis. Negative values represent overbound complexes. (Bottom) Absolute value of basis set errors plotted on a logarithmic axis.

interaction energies are combined with several correction factors (thermal corrections, ZPVE, entropy corrections, etc); however, this does not remove the fact that the CP correction changes the final result by 15.2 kcal/mol. For calculations that desire to approach chemical accuracy (±1 kcal/mol), a correction factor of this magnitude becomes problematic, unless one can show that the CP correction brings the electronic interaction energy closer to the value expected for a *complete* basis set. However, our MW-computed electronic interaction energy for reaction Ni–alkene-3 is −6.7 kcal/mol, which is approximately in the middle between the uncorrected 6-311G(d,p) energy (−14.0 kcal/mol, error −7.3 kcal/mol) and the CP-corrected value (+1.2, error +7.9 kcal/mol). This lends some support to previous proposals to use half the counterpoise correction;[108,110] however, we do note that the underbinding caused by the full CP correction is highly basis set- and ligand-dependent, and thus, a general reduction of the CP to 50% cannot be recommended.

On basis of the overall results in Figs. 2–5, we can conclude that on average, BSSEs of 2–9 kcal/mol can be observed for metal–ligand interactions for widely used medium-sized basis sets and that CP corrections do not consistently improve results. It is important to note that is it impossible to know for a given reaction and a given basis set if the CP correction will provide improved results or not. A general recommendation may thus be to not use CP corrections but rather to use larger GTO basis sets for single point energies or, in order to avoid BSEs altogether, to use MWs.

C. A closer look at 6-311G(d,p)

The poor performance of 6-311G(d,p) stands out from several of the results presented in Secs. III A and III B. It displays BSSEs that more resemble DZ basis sets than TZ basis sets, both in kcal/mol and relative to the interaction energy (Figs. 2 and 3). Looking at Fig. 5, one sees that to a large extent, the 6-311G(d,p) CP correction leads to an underbinding to about the same extent as the uncorrected values overbind. In other words, one might as well not have performed the correction. Of course, the CP correction's job is not to bring the interaction energy closer to the CBS limit, but rather to remove the BSSE. Whether or not the resulting interaction energy is closer to

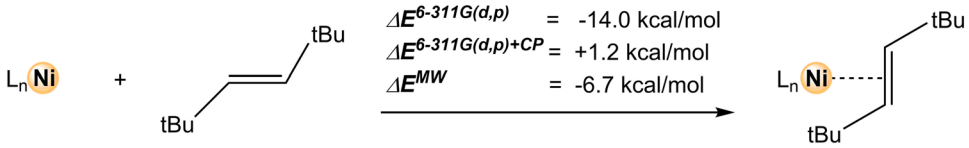

SCHEME 4. Reaction Ni–alkene-3 and the 6-311G(d,p) electronic reaction energy with and without CP correction, alongside the complete basis set multiwavelet (MW7) electronic interaction energy (all PBE).

the CBS limit depends on the interplay between BSSEs and BSIEs. However, the premise for applying the CP correction is that it leads to more robust interaction energies, but this does not seem to be the case for 6-311G(d,p). Table III illustrates several examples. For the Cr reactions, the errors of up to −6.69 kcal/mol in the 6-311G(d,p) interaction energies are reduced to errors of up to +1.59 kcal/mol after application of the CP correction, implying that the results seem reasonable, although a consistent underestimation of the interaction energy (i.e., underbinding) is observed for the CP-corrected values. For the Ni reactions, the CP-overcorrection is much more severe, and in some cases, it even reverses the sign of the electronic reaction energy (e.g., Ni–alkene-3, Ni–alkene-5, Ni–water, Table III). The BSE of the CP-corrected energies is between 6 and 10 kcal/mol for all Ni reactions. This ill behavior for the Ni reactions is not observed for other basis sets [except 6-311G, which shares the poor performance of 6-311G(d,p)], and even the smaller DZ Pople basis sets give more uniform deviations from the CBS reference.

Plotting the BSEs as a function of the number of basis functions used to describe the transition metal complexes (Fig. 6), one sees that 6-311G(d,p) indeed should be considered a double-ζ basis set in practice, despite formally being a triple-ζ basis set. The same is observed if one instead plots the BSSEs as a function of the basis set size (supplementary material, Fig. S17). A similar conclusion was reached by Grev and Schaefer, who argued that the second set of the three contracted *s*-functions in 6-311G is not a valence orbital but a 1*s* function, turning the basis set, in practice, into 63-11G.[111] It can be noted that the 6-311G(d,p) basis set nonetheless is used in many contemporary studies for computing reaction energies of metal systems.[31,33,112–114] On the basis of the shortcomings described here, it is strongly recommended to not use this basis set for computing energies, at least not for DFT-studies on the type of transition metal-based systems considered here.

D. Convenience of MWs to compute organometallic reaction energies

The combined results for 26 association reactions show that the basis set error in commonly used GTO basis sets can be large (Figs. 2–5). In order to reduce the BSE, one could use a large GTO basis, such as the QZ basis set pc-3. However, if one desires to quantify the remaining BSSE in large GTO calculations using

TABLE III. Interaction energies (in kcal/mol) from uncorrected and CP-corrected 6-311G(d,p) calculations, compared to our MW7 reference values (all PBE). The 6-311G(d,p) basis set performs significantly worse than other TZ basis sets, and adding a CP correction does not seem to robustly improve the interaction energies and even changes the sign of the electronic reaction energy in several cases.

Reaction	ΔE 6-311G(d,p)	ΔE 6-311G(d,p) + CP	ΔE MW7	BSE 6-311G(d,p)[a]	BSE 6-311G(d,p) + CP[a]
Cr–alkene-1	−28.1338	−24.1678	−24.9850	−3.15	+0.82
Cr–alkene-2	−25.2397	−20.1590	−20.6987	−4.54	+0.54
Cr–alkene-3	−15.1441	−8.3921	−9.6207	−5.52	+1.23
Cr–alkene-4	−21.1783	−14.9975	−15.8985	−5.28	+0.90
Cr–alkene-5	−15.2103	−8.3959	−9.9841	−5.23	+1.59
Cr–alkene-6	−21.8598	−15.2904	−16.3504	−5.51	+1.06
Cr–water	−23.2986	−17.0040	−16.6123	−6.69	−0.39
Cr–MeOH	−23.3927	−17.9786	−18.1595	−5.23	+0.18
Cr–THF	−24.1624	−19.0998	−19.5419	−4.62	+0.44
Cr–MeCN	−32.5058	−28.5472	−29.4296	−3.08	+0.88
Cr–CO	−46.6358	−42.7000	−43.7583	−2.88	+1.06
Cr–H2	−19.5768	−17.8168	−19.0923	−0.48	+1.28
Ni–alkene-1	−20.6416	−7.1626	−16.3267	−4.31	+9.16
Ni–alkene-2	−16.5817	−4.5109	−11.9557	−4.63	+7.44
Ni–alkene-3	−14.0039	+1.1945	−6.6447	−7.36	+7.84
Ni–alkene-4	−13.9730	−1.5440	−8.9230	−5.05	+7.38
Ni–alkene-5	−12.4233	+1.6408	−6.3232	−6.10	+7.96
Ni–alkene-6	−14.4654	−1.8928	−9.1713	−5.29	+7.28
Ni–water	−8.3520	+0.0439	−5.9256	−2.43	+5.97
Ni–MeOH	−9.3419	−0.7937	−7.1498	−2.19	+6.36
Ni–THF	−10.3608	−1.3775	−8.0951	−2.27	+6.72
Ni–MeCN	−16.2620	−8.0467	−15.9414	−0.32	+7.89
Ni–CO	−30.4033	−19.1056	−29.2362	−1.17	+10.13
Ni–NHC-1	−41.7440	−27.6821	−36.5822	−5.16	+8.90
Ni–NHC-2	−43.8376	−27.7610	−36.0936	−7.74	+8.33
Fe–MeOH	−21.9143	−14.6955	−14.4696	−7.44	−0.23

[a]Basis set error of GTO calculation relative to the complete basis set limit, computed as ΔE[GTO] − ΔE[MW7].

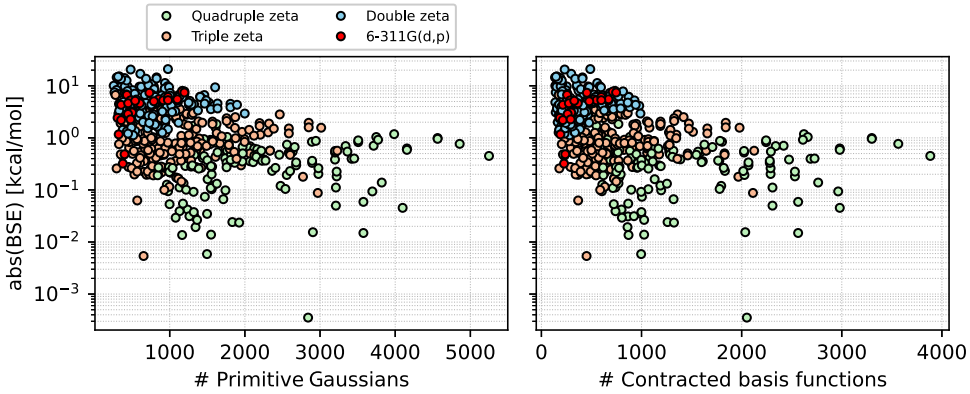

FIG. 6. Basis set errors (BSEs) plotted against the number of *primitive* Gaussian basis functions on the complex (left) and against the number of *contracted* basis functions of the product complex (right) for all GTO basis sets evaluated here (all PBE). 6-311G(d,p) is plotted by itself (in red) and is seen to cluster together with DZ basis sets rather than TZ basis sets with respect to basis set errors and size.

the counterpoise method, this can become very cumbersome. For example, consider a chemical transformation, such as an insertion into a metal–ligand bond (Fig. 7, left). For such instances, it is not straightforward to use the counterpoise correction to compute the BSSE arising from the combination of the fragments in A to give complex C. Unfortunately, in organometallic chemistry, one is very often faced with reaction steps where a change in number of moles occurs simultaneously with a chemical transformation. A possible work-around to compute the CP is present if an intermediate structure B exists, for which the CP can be computed (Fig. 7). However, this provides only an approximation of the BSSE present in structure C relative to A. An alternative and straightforward solution is to use MWs instead of large GTOs. In this case, one only has to compute the single point MW energies on states A and C, no additional CP calculations are needed, and no work-around via structure B has to be attempted. Furthermore, the computed MW and pc-n results for the Ni–O_2CMe reaction (Fig. 7, right) indicate that the approximate CP correction does not consistently reduce the BSE. Still, the overall performance of the pc-n series seems very good for this case, with an absolute BSE less than ~0.1 kcal/mol already at the pc-2 level, which is much smaller than other error contributions in current DFT calculations. However, there is no clear trend or systematic improvement of the results when going beyond pc-2, and the very large pc-4 basis is just as far from the MW reference as pc-2. It can be noted that MWs have only recently become able to compute metal systems (and to our knowledge, this paper is the first report of MW calculations on transition metal complexes), so their implementation and timings are not yet on par with large GTO basis sets (see supplementary material, Table S2 for timings for reaction Ni–O_2CMe). However, future developments will improve these timings and allow the extension of MW calculations to all elements in the Periodic Table.

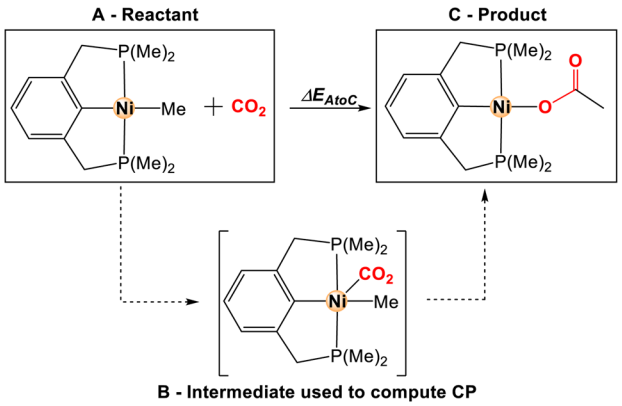

Computed electronic reaction energies for reaction Ni-O_2CMe

	ΔE Hartree	ΔE kcal/mol	BSE kcal/mol	Error rel. MW %
ΔE_{AtoC}^{pc-1}	-0.038806	-24.35	-3.63	17.49
$\Delta E_{AtoC}^{pc-1+CP}$	-0.035414	-22.22	-1.50	7.22
ΔE_{AtoC}^{pc-2}	-0.033179	-20.82	-0.09	0.46
$\Delta E_{AtoC}^{pc-2+CP}$	-0.032559	-20.43	0.29	1.42
ΔE_{AtoC}^{pc-3}	-0.033108	-20.78	-0.05	0.24
$\Delta E_{AtoC}^{pc-3+CP}$	-0.033053	-20.74	-0.01	0.05
ΔE_{AtoC}^{pc-4}	-0.033156	-20.81	-0.08	0.39
$\Delta E_{AtoC}^{pc-4+CP}$	-0.033155	-20.80	-0.08	0.38
ΔE_{AtoC}^{MW6}	-0.033028	-20.73	-	-

FIG. 7. (Left) Reaction Ni–O_2CMe, involving insertion of CO_2 into a Ni–Me bond. In order to compute the CP correction with GTO basis sets, intermediate B can be used as an approximation, if it exists. (Right) Computed electronic reaction energies for reaction Ni–O_2CMe with pc-1 (double-ζ), pc-2 (triple-ζ), pc-3 (quadruple-ζ), and pc-4 (quintuple-ζ) GTO basis sets, with and without CP correction (from structure B) compared to MW6 results.

IV. CONCLUSIONS

We have presented high-precision Multiwavelet (MW) energies for 26 transition metal-mediated reactions involving association of common ligands, such as H_2, CO, olefins, or solvent molecules (Scheme 1). By comparing the MW results, we have shown that commonly used DZ and TZ GTO basis sets can have large basis set errors. For the tested triple-ζ basis sets, the average absolute BSEs are up to 5.0 kcal/mol for the Pople basis sets, 1.4 kcal/mol for Dunning basis sets, 0.8 kcal/mol for Ahlrichs basis sets, and 0.5 kcal/mol for Jensen basis sets (Table II). Using the counterpoise method to correct for BSSEs leads to underbinding in many cases (Fig. 5). A particular poor example is the formally triple-ζ Pople basis set 6-311G(d,p), which should be considered a double-ζ basis set in practice (Figure 6)[111] and which we do not recommend for computing energies.

The results presented here showcase the large variance in electronic interaction energies one can expect for the same reaction step computed with different GTO basis sets. Due to the particular balance of the errors inherent to each basis set, GTO results contain large uncertainties. It is also important to note that reaction steps of different chemical nature may provide very different errors. If one considers the mechanism for a catalytic cycle, each step in the cycle may be chemically distinct (e.g., association, reductive elimination, migratory insertion, and metathesis). A single GTO basis set may not be able to describe each step in the cycle on equal footing, which can lead to unpredictable errors when evaluating relative energies. Thus, the computed energy for an intermolecular association step may easily have an error of more than 10 kcal/mol (as indicated by the large BSSEs observed in our study, Fig. 3), but one can expect that a following intramolecular step may have a much smaller error. This type of uncertainty may not be obvious to the non-expert, as it is easy to think of a basis set's description as uniform across different elementary reaction steps.

MWs converge toward the exact CBS limit to within a predefined precision set by the user. This guarantees a uniform basis set description regardless of the chemical system, implying that MWs conveniently can be applied to any type of reaction. It also eliminates any interplay between the basis set and the DFT functional, allowing a user to evaluate a functional's inherent accuracy without considering DFT errors being canceled by basis set errors. As illustrated by the aug-pc-3 results (Fig. S18 in the supplementary material), the CBS limit convergence can effectively be precluded for GTO basis sets due to numerical issues generated by near-linear dependencies. MWs are orthonormal by construction and such issues cannot arise. Thus, MWs constitute a highly promising basis, both for applications to any type of properties and for use in development of new methodologies, such as new DFT functionals.

SUPPLEMENTARY MATERIAL

See the supplementary material for results with additional basis sets and DFT functionals and for optimized coordinates.

DEDICATION

This paper is dedicated to Ingrid Daubechies, a Belgian physicist and mathematician, whose pioneering work on wavelets opened new avenues in computational physics and chemistry.

ACKNOWLEDGMENTS

This work was supported by a Centre of Excellence grant (No. 262695), by the Tromsø Research Foundation (Grant No. TFS2016KHH), and by UNINETT Sigma2 through grants of computer time (Grant Nos. nn9330k and nn4654k). We thank Dr. Diego Garcia-Lopez for the input coordinates of the Ni–pincer complex. We gratefully thank Dr. Susi Lehtola for bringing Ref. 111 to our attention.

DATA AVAILABILITY

The data that support the findings of this study are openly available in DataverseNO at https://doi.org/10.18710/WA5YCF, Ref. 116, and from the corresponding author upon reasonable request.

REFERENCES

[1]H. Ryu, J. Park, H. K. Kim, J. Y. Park, S.-T. Kim, and M.-H. Baik, "Pitfalls in computational modeling of chemical reactions and how to avoid them," Organometallics **37**, 3228 (2018).
[2]I. Funes-Ardoiz and F. Schoenebeck, "Established and emerging computational tools to study homogeneous catalysis—From quantum mechanics to machine learning," Chem **6**, 1904 (2020).
[3]G. Sciortino, S. Muñoz-López, A. Lledós, and G. Ujaque, "Comparative mechanistic study on the $[Au(NHC)]^+$-catalyzed hydration of alkynes, alkenes, and allenes," Organometallics **39**, 3469 (2020).
[4]N. X. Gu, P. H. Oyala, and J. C. Peters, "H_2 evolution from a thiolate-bound Ni(III) hydride," J. Am. Chem. Soc. **142**, 7827 (2020).
[5]M. Isegawa, T. Matsumoto, and S. Ogo, "Selective oxidation of H_2 and CO by NiIr catalyst in aqueous solution: A DFT mechanistic study," Inorg. Chem. **59**, 1014 (2020).
[6]C. Mealli, G. Manca, R. Tarroni, D. Olivieri, and C. Carfagna, "Computational overview of a Pd-catalyzed olefin Bis-alkoxycarbonylation process," Organometallics **39**, 1059 (2020).
[7]M. Sparta, C. Riplinger, and F. Neese, "Mechanism of olefin asymmetric hydrogenation catalyzed by iridium phosphino-oxazoline: A pair natural orbital coupled cluster study," J. Chem. Theory Comput. **10**, 1099 (2014).
[8]D. Hong, Y. Shimoyama, Y. Ohgomori, R. Kanega, H. Kotani, T. Ishizuka, Y. Kon, Y. Himeda, and T. Kojima, "Cooperative effects of heterodinuclear Ir^{III}–M^{II} complexes on catalytic H_2 evolution from formic acid dehydrogenation in water," Inorg. Chem. **59**, 11976 (2020).
[9]Y. Luo, Z. Huang, Z. Chen, Z. Xu, J. Meng, H.-Y. Li, Q. Meng, and D. Tang, "Strategy used to control the mechanism of homogeneous alkyne/olefin hydrogenation: AIMD simulations and DFT calculations," J. Org. Chem. **85**, 11626 (2020).
[10]N. Li, R. Chang, W. Yang, Z. Zhang, and Z. Guo, "Mechanistic insights into Ni-catalyzed difunctionalization of alkenes using organoboronic acids and organic halides: Understanding remarkable substrate-dependent regioselectivity," Organometallics **39**, 2057 (2020).
[11]N. Sieffert and M. Bühl, "Noncovalent interactions in a transition-metal triphenylphosphine complex: A density functional case study," Inorg. Chem. **48**, 4622 (2009).
[12]M. M. Quintal, A. Karton, M. A. Iron, A. D. Boese, and J. M. L. Martin, "Benchmark study of DFT functionals for late-transition-metal reactions," J. Phys. Chem. A **110**, 709 (2006).
[13]Y. Minenkov, G. Occhipinti, and V. R. Jensen, "Metal–phosphine bond strengths of the transition metals: A challenge for DFT," J. Phys. Chem. A **113**, 11833 (2009).
[14]M. Sparta, V. R. Jensen, and K. J. Børve, "Accurate metal–ligand bond energies in the η^2-C_2H_4 and η^2-C_{60} complexes of $Pt(PH_3)_2$, with application to their Bis(triphenylphosphine) analogues," Mol. Phys. **111**, 1599 (2013).

[15]T. Husch, L. Freitag, and M. Reiher, "Calculation of ligand dissociation energies in large transition-metal complexes," J. Chem. Theory Comput. **14**, 2456 (2018).
[16]B. A. Shiekh, "Hierarchy of commonly used DFT methods for predicting the thermochemistry of Rh-mediated chemical transformations," ACS Omega **4**, 15435 (2019).
[17]M. A. Iron and T. Janes, "Evaluating transition metal barrier heights with the latest density functional theory exchange–correlation functionals: The MOBH35 benchmark database," J. Phys. Chem. A **123**, 3761 (2019).
[18]M. Modrzejewski, G. Chalasinski, and M. M. Szczesniak, "Assessment of newest meta-GGA hybrids for late transition metal reactivity: Fractional charge and fractional spin perspective," J. Phys. Chem. C **123**, 8047 (2018).
[19]S. Dohm, A. Hansen, M. Steinmetz, S. Grimme, and M. P. Checinski, "Comprehensive thermochemical benchmark set of realistic closed-shell metal organic reactions," J. Chem. Theory Comput. **14**, 2596 (2018).
[20]Y. A. Aoto, A. P. de Lima Batista, A. Köhn, and A. G. S. de Oliveira-Filho, "How to arrive at accurate benchmark values for transition metal compounds: Computation or experiment?," J. Chem. Theory Comput. **13**, 5291 (2017).
[21]T. Weymuth, E. P. A. Couzijn, P. Chen, and M. Reiher, "New benchmark set of transition-metal coordination reactions for the assessment of density functionals," J. Chem. Theory Comput. **10**, 3092 (2014).
[22]M. Steinmetz and S. Grimme, "Benchmark study of the performance of density functional theory for bond activations with (Ni,Pd)-based transition-metal catalysts," ChemistryOpen **2**, 115 (2013).
[23]Á. Vidal Vidal, L. C. de Vicente Poutás, O. Nieto Faza, and C. S. López, "On the use of popular basis sets: Impact of the intramolecular basis set superposition error," Molecules **24**, 3810 (2019).
[24]C. Plascencia, J. Wang, and A. K. Wilson, "Importance of the ligand basis set in *ab initio* thermochemical calculations of transition metal species," Chem. Phys. Lett. **685**, 496 (2017).
[25]R. Sure, J. G. Brandenburg, and S. Grimme, "Small atomic orbital basis set first-principles quantum chemical methods for large molecular and periodic systems: A critical analysis of error sources," ChemistryOpen **5**, 94 (2016).
[26]W. J. Hehre, R. Ditchfield, and J. A. Pople, "Self-consistent molecular orbital methods. XII. Further extensions of Gaussian—type basis sets for use in molecular orbital studies of organic molecules," J. Chem. Phys. **56**, 2257 (1972).
[27]F. Weigend and R. Ahlrichs, "Balanced basis sets of split valence, triple zeta valence and quadruple zeta valence quality for H to Rn: Design and assessment of accuracy," Phys. Chem. Chem. Phys. **7**, 3297 (2005).
[28]K. Lee, J. D. Culpepper, R. Parveen, D. C. Swenson, B. Vlaisavljevich, and S. R. Daly, "Modifying phosphorus(III) substituents to activate remote ligand-centered reactivity in triaminoborane ligands," Organometallics **39**, 2526 (2020).
[29]S. Ghorai and E. D. Jemmis, "DFT study of C–C and C–N coupling on a quintuple-bonded Cr_2 template: MECP (minimum energy crossing point) barriers control product distribution," Organometallics **39**, 1700 (2020).
[30]K. Sakata and S. Shimada, and R. Takeuchi, "Regioselectivity in the iridium-catalyzed [2 + 2 + 2] cycloaddition of unsymmetrical α,ω-diynes with nitrile: A DFT study," Organometallics **39**, 2091 (2020).
[31]I. G. Powers, J. M. Andjaba, M. Zeller, and C. Uyeda, "Catalytic C(sp^2)–H amination reactions using dinickel imides," Organometallics **39**, 3794 (2020).
[32]G. Keglevich, R. Henyecz, and Z. Mucsi, "Experimental and theoretical study on the '2,2′-bipiridyl-Ni-catalyzed' Hirao reaction of >P(O)H reagents and halobenzenes: A Ni(0) → Ni(II) or a Ni(II) → Ni(IV) mechanism?," J. Org. Chem. **85**, 14486 (2020).
[33]C. Maquilón, B. Limburg, V. Laserna, D. Garay-Ruiz, J. González-Fabra, C. Bo, M. Martínez Belmonte, E. C. Escudero-Adán, and A. W. Kleij, "Effect of an Al(III) complex on the regio- and stereoisomeric formation of bicyclic organic carbonates," Organometallics **39**, 1642 (2020).
[34]A. Winkler, K. Brandhorst, M. Freytag, P. G. Jones, and M. Tamm, "Palladium(II) complexes with anionic N-heterocyclic carbene–borate ligands as catalysts for the amination of aryl halides," Organometallics **35**, 1160 (2016).
[35]V. Varela-Izquierdo, A. M. Geer, J. Navarro, J. A. López, M. A. Ciriano, and C. Tejel, "Rhodium complexes in P–C bond formation: Key role of a hydrido ligand," J. Am. Chem. Soc. **143**, 349 (2021).
[36]A. M. Camp, M. R. Kita, P. T. Blackburn, H. M. Dodge, C.-H. Chen, and A. J. M. Miller, "Selecting double bond positions with a single cation-responsive iridium olefin isomerization catalyst," J. Am. Chem. Soc. **143**, 2792 (2021).
[37]L. A. Hammarback, B. J. Aucott, J. T. W. Bary, I. P. Clark, M. Towrie, A. Robinson, I. J. S. Fairlamb, and J. M. Lynam, "Direct observation of the microscopic reverse of the ubiquitous concerted metalation deprotonation step in C–H bond activation catalysis," J. Am. Chem. Soc. **143**, 1356 (2021).
[38]Z. Bai, H. Zhang, H. Wang, H. Yu, G. Chen, and G. He, "Enantioselective alkylamination of unactivated alkenes under copper catalysis," J. Am. Chem. Soc. **143**, 1195 (2021).
[39]L. Zhao, C. Hu, X. Cong, G. Deng, L. L. Liu, M. Luo, and X. Zeng, "Cyclic (alkyl)(amino)carbene ligand-promoted nitro deoxygenative hydroboration with chromium catalysis: Scope, mechanism, and applications," J. Am. Chem. Soc. **143**, 1618 (2021).
[40]H. Shao, S. Chakrabarty, X. Qi, J. M. Takacs, and P. Liu, "Ligand conformational flexibility enables enantioselective tertiary C–B bond formation in the phosphonate-directed catalytic asymmetric alkene hydroboration," J. Am. Chem. Soc. **143**, 4801 (2021).
[41]In a small literature survey, we found that only 2 of 26 recently published articles in the Journal of the American Chemical Society (all from 2021) employed correlation consistent basis sets for computing energies of transition-metal systems. An example includes M. Kim, B. Park, M. Shin, S. Kim, J. Kim, M.-H. Baik, and S. H. Cho, "Copper-catalyzed enantiotopic-group-selective allylation of gem-diborylalkanes," J. Am. Chem. Soc. **143**, 1069 (2021).
[42]H. Kruse and S. Grimme, "A geometrical correction for the inter- and intramolecular basis set superposition error in Hartree–Fock and density functional theory calculations for large systems," J. Chem. Phys. **136**, 154101 (2012).
[43]S. F. Boys and F. Bernardi, "The calculation of small molecular interactions by the differences of separate total energies. Some procedures with reduced errors," Mol. Phys. **19**, 553 (1970).
[44]F. B. van Duijneveldt, J. G. C. M. van Duijneveldt-van de Rijdt, and J. H. van Lenthe, "State of the art in counterpoise theory," Chem. Rev. **94**, 1873 (1994).
[45]The BSSE is usually divided into two subcategories: inter- and intramolecular BSSE. While both types originate from the same principles (overlapping basis functions), they differ in the remedies used to correct for them. It is beyond the scope of this paper to review strategies for dealing with intramolecular BSSEs.
[46]B. Brauer, M. K. Kesharwani, and J. M. L. Martin, "Some observations on counterpoise corrections for explicitly correlated calculations on noncovalent interactions," Chem. Theory Comput. **10**, 3791 (2014).
[47]J. Witte, J. B. Neaton, and M. Head-Gordon, "Push it to the limit: Characterizing the convergence of common sequences of basis sets for intermolecular interactions as described by density functional theory," J. Chem. Phys. **144**, 194306 (2016).
[48]S. Shafiei-Haghighi, A. Brar, D. K. Unruh, A. F. Cozzolino, and M. Findlater, "Experimental and computational studies of phosphine ligand displacement in iridium–pincer complexes employing pyridine or acetonitrile," Organometallics **39**, 3461 (2020).
[49]B. L. Oliveira, B. J. Stenton, V. B. Unnikrishnan, C. R. de Almeida, J. Conde, M. Negrão, F. S. S. Schneider, C. Cordeiro, M. G. Ferreira, G. F. Caramori, J. B. Domingos, R. Fior, and G. J. L. Bernardes, "Platinum-triggered bond-cleavage of pentynoyl amide and *N*-propargyl handles for drug-activation," J. Am. Chem. Soc. **142**, 10869 (2020).
[50]M. Gutowski, J. H. van Lenthe, J. Verbeek, F. B. van Duijneveldt, and G. Chałasinski, "The basis set superposition error in correlated electronic structure calculations," Chem. Phys. Lett. **124**, 370 (1986).
[51]M. M. Szczęèniak and S. Scheiner, "Correction of the basis set superposition error in SCF and MP2 interaction energies. The water dimer," J. Chem. Phys. **84**, 6328 (1986).
[52]S. M. Tekarli, M. L. Drummond, T. G. Williams, T. R. Cundari, and. A. K. Wilson, "Performance of density functional theory for 3d transition metal-containing complexes: Utilization of the correlation consistent basis sets," J. Phys. Chem. A **113**, 8607 (2009).
[53]L. Frediani and D. Sundholm, "Real-space numerical grid methods in quantum chemistry," Phys. Chem. Chem. Phys. **17**, 31357 (2015).
[54]B. Alpert, G. Beylkin, D. Gines, and L. Vozovoi, "Adaptive solution of partial differential equations in multiwavelet bases," J. Comput. Phys. **182**, 149 (2002).

[55]B. K. Alpert, "A class of bases in L^2 for the sparse representation of integral operators," SIAM J. Math. Anal. **24**, 246 (1993).
[56]L. Frediani, E. Fossgaard, T. Flå, and K. Ruud, "Fully adaptive algorithms for multivariate integral equations using the non-standard form and multiwavelets with applications to the Poisson and bound-state Helmholtz kernels in three dimensions," Mol. Phys. **111**, 1143 (2013).
[57]R. J. Harrison, G. I. Fann, T. Yanai, Z. Gan, and G. Beylkin, "Multiresolution quantum chemistry: Basic theory and initial applications," J. Chem. Phys. **121**, 11587 (2004).
[58]T. Yanai, G. I. Fann, Z. Gan, R. J. Harrison, and G. Beylkin, "Multiresolution quantum chemistry in multiwavelet bases: Hartree–Fock exchange," J. Chem. Phys. **121**, 6680 (2004).
[59]T. Yanai, G. I. Fann, Z. Gan, R. J. Harrison, and G. Beylkin, "Multiresolution quantum chemistry in multiwavelet bases: Analytic derivatives for Hartree–Fock and density functional theory," J. Chem. Phys. **121**, 2866 (2004).
[60]G. Beylkin, V. Cheruvu, and F. Perez, "Fast adaptive algorithms in the non-standard form for multidimensional problems," Appl. Comput. Harmonic Anal. **24**, 354 (2008).
[61]M. H. Kalos, "Monte Carlo calculations of the ground state of three- and four-body nuclei," Phys. Rev. **128**, 1791 (1962).
[62]G. Beylkin, R. Cramer, G. Fann, and R. J. Harrison, "Multiresolution separated representations of singular and weakly singular operators," Appl. Comput. Harmonic Anal. **23**, 235 (2007).
[63]S. R. Jensen, S. Saha, J. A. Flores-Livas, W. Huhn, V. Blum, S. Goedecker, and L. Frediani, "The elephant in the room of density functional theory calculations," J. Phys. Chem. Lett. **8**, 1449 (2017).
[64]A. Brakestad, S. R. Jensen, P. Wind, M. D'Alessandro, L. Genovese, K. H. Hopmann, and L. Frediani, "Static polarizabilities at the basis set limit: A benchmark of 124 species," J. Chem. Theory Comput. **16**, 4874 (2020).
[65]S. R. Jensen, T. Flå, D. Jonsson, R. S. Monstad, K. Ruud, and L. Frediani, "Magnetic properties with multiwavelets and DFT: The complete basis set limit achieved," Phys. Chem. Chem. Phys. **18**, 21145 (2016).
[66]Á. Vázquez-Mayagoitia, W. S. Thornton, J. R. Hammond, and R. J. Harrison, "Quantum chemistry methods with multiwavelet bases on massive parallel computers," Annu. Rep. Comput. Chem. **10**, 3 (2014).
[67]L. A. Barnes, B. Liu, and R. Lindh, "Structure and energetics of $Cr(CO)_6$ and $Cr(CO)_5$," J. Chem. Phys. **98**, 3978 (1993).
[68]G. R. Morello and K. H. Hopmann, "A dihydride mechanism can explain the intriguing substrate selectivity of iron-PNP-mediated hydrogenation," ACS Catal. **7**, 5847 (2017).
[69]F. Neese, "Software update: The ORCA program system, version 4.0," Wiley Interdiscip. Rev.: Comput. Mol. Sci. **8**, e1327 (2017).
[70]F. Neese, F. Wennmohs, U. Becker, and C. Riplinger, "The ORCA quantum chemistry program package," J. Chem. Phys. **152**, 224108 (2020).
[71]P. Hohenberg and W. Kohn, "Inhomogeneous electron gas," Phys. Rev. **136**, B864 (1964).
[72]W. Kohn and L. J. Sham, "Self-consistent equations including exchange and correlation effects," Phys. Rev. **140**, A1133 (1965).
[73]E. J. Baerends, D. E. Ellis, and P. Ros, "Self-consistent molecular Hartree—Fock—Slater calculations I. The computational procedure," Chem. Phys. **2**, 41 (1973).
[74]J. L. Whitten, "Coulombic potential energy integrals and approximations," J. Phys. Chem. **58**, 4496 (1973).
[75]B. I. Dunlap, J. W. D. Connolly, and J. R. Sabin, "On some approximations in applications of $X\alpha$ theory," J. Chem. Phys. **71**, 3396 (1979).
[76]C. van Alsenoy, "*Ab initio* calculations on large molecules: The multiplicative integral approximation," J. Comput. Chem. **9**, 620 (1988).
[77]K. Eichkorn, F. Weigend, O. Treutler, and R. Ahlrichs, "Auxiliary basis sets for main row atoms and transition metals and their use to approximate Coulomb potentials," Theor. Chem. Acta **97**, 119 (1997).
[78]R. A. Kendall and H. A. Früchtl, "The impact of the resolution of the identity approximate integral method on modern ab initio algorithm development," Theor. Chem. Acta **97**, 158 (1997).
[79]D. E. Bernholdt and R. J. Harrison, "Fitting basis sets for the RI-MP2 approximate second-order many-body perturbation theory method," J. Chem. Phys. **109**, 1593 (1998).
[80]S. Grimme, J. Antony, S. Ehrlich, and H. Krieg, "A consistent and accurate *ab initio* parametrization of density functional dispersion correction (DFT-d) for the 94 elements H-Pu," J. Chem. Phys. **132**, 154104 (2010).
[81]S. Grimme, S. Ehrlich, and L. Goerigk, "Effect of the damping function in dispersion corrected density functional theory," J. Comput. Chem. **32**, 1456 (2011).
[82]J. P. Perdew, "Erratum: Density-functional approximation for the correlation energy of the inhomogeneous electron gas," Phys. Rev. B **34**, 7406 (1986).
[83]J. P. Perdew, "Density-functional approximation for the correlation energy of the inhomogeneous electron gas," Phys. Rev. B **33**, 8822 (1986).
[84]A. D. Becke, "Density-functional exchange-energy approximation with correct asymptotic behavior," Phys. Rev. A **38**, 3098 (1988).
[85]C. Adamo and V. Barone, "Toward reliable density functional methods without adjustable parameters: The PBE0 model," J. Chem. Phys. **110**, 6158 (1999).
[86]M. Ernzerhof and G. E. Scuseria, "Assessment of the Perdew–Burke–Ernzerhof exchange-correlation functional," J. Chem. Phys. **110**, 5029 (1999).
[87]F. Jensen, "Polarization consistent basis sets: Principles," J. Chem. Phys. **115**, 9113 (2001).
[88]F. Jensen, "Polarization consistent basis sets: II. Estimating the Kohn–Sham basis set limit," J. Chem. Phys. **116**, 7372 (2002).
[89]F. Jensen, "Polarization consistent basis sets. III. The importance of diffuse functions," J. Chem. Phys. **117**, 9234 (2002).
[90]F. Jensen and T. Helgaker, "Polarization consistent basis sets. V. The elements Si–Cl," J. Chem. Phys. **121**, 3463 (2004).
[91]T. H. Dunning, "Gaussian basis sets for use in correlated molecular calculations. I. The atoms boron through neon and hydrogen," J. Chem. Phys. **90**, 1007 (1989).
[92]D. E. Woon and T. H. Dunning, "Gaussian basis sets for use in correlated molecular calculations. III. The atoms aluminum through argon," J. Chem. Phys. **98**, 1358 (1993).
[93]N. B. Balabanov and K. A. Peterson, "Systematically convergent basis sets for transition metals. I. All electron correlation consistent basis sets for the 3*d* elements Sc–Zn," J. Chem. Phys. **123**, 064107 (2005).
[94]N. B. Balabanov and K. A. Peterson, "Basis set limit electronic excitation energies, ionization potentials, and electron affinities for the 3*d* transition metal atoms: Coupled cluster and multireference methods," J. Chem. Phys. **125**, 074110 (2006).
[95]R. Krishnan, J. S. Binkley, R. Seeger, and J. A. Pople, "Self-consistent molecular orbital methods. XX. A basis set for correlated wave functions," J. Chem. Phys. **72**, 650 (1980).
[96]A. D. McLean and G. S. Chandler, "Contracted Gaussian basis sets for molecular calculations. I. Second row atoms, z=11–18," J. Chem. Phys. **72**, 5639 (1980).
[97]M. M. Francl, W. J. Pietro, W. J. Hehre, J. S. Binkley, M. S. Gordon, D. J. DeFrees, and J. A. Pople, "Self-consistent molecular orbital methods. XXIII. A polarization-type basis set for second-row elements," J. Chem. Phys. **77**, 3654 (1982).
[98]T. Clark, J. Chandrasekhar, G. W. Spitznagel, and P. V. R. Schleyer, "Efficient diffuse function-augmented basis sets for anion calculations. III. The 3-21+G basis set for first-row elements, Li–F," J. Comput. Chem. **4**, 294 (1983).
[99]M. J. Frisch, J. A. Pople, and J. S. Binkley, "Self-consistent molecular orbital methods 25. Supplementary functions for Gaussian basis sets," J. Chem. Phys. **80**, 3265 (1984).
[100]L. A. Curtiss, M. P. McGrath, J. P. Blaudeau, N. E. Davis, R. C. Binning, and L. Radom, "Extension of Gaussian-2 theory to molecules containing third-row atoms Ga–Kr," J. Chem. Phys. **103**, 6104 (1995).
[101]J.-P. Blaudeau, M. P. McGrath, L. A. Curtiss, and L. Radom, "Extension of Gaussian-2 (G2) theory to molecules containing third-row atoms K and Ca," J. Chem. Phys. **107**, 5016 (1997).
[102]V. A. Rassolov, J. A. Pople, M. A. Ratner, and T. L. Windus, "6-31G* basis set for atoms K through Zn," J. Chem. Phys. **109**, 1223 (1998).
[103]P. J. Hay and W. R. Wadt, "*Ab initio* effective core potentials for molecular calculations. Potentials for K to Au including the outermost core orbitals," J. Chem. Phys. **82**, 299 (1985).

[104]R. Bast, M. Bjorgve, R. Di Remigio, A. Durdek, L. Frediani, G. Gerez, S. R. Jensen, J. Juselius, R. Monstad, and P. Wind (2020). "MRChem: MultiResolution Chemistry," Zenodo. https://doi.org/10.5281/zenodo.4306059.
[105]See https://mrchem.readthedocs.io/en/latest for MRChem Documentation, 2020.
[106]R. J. Harrison, "Krylov subspace accelerated inexact Newton method for linear and nonlinear equations," J. Comput. Chem **25**, 328 (2003).
[107]If there are few basis functions, these are less likely to overlap, which is the reason for the small BSSE of minimal basis sets. Note that a small BSSE does not imply a good basis set, as the overall BSE will be large for minimal basis sets.
[108]K. S. Kim, P. Tarakeshwar, and J. Y. Lee, "Molecular clusters of π-systems: Theoretical studies of structures, spectra, and origin of interaction energies," Chem. Rev. **100**, 4145 (2000).
[109]J. Diccianni, Q. Lin, and T. Diao, "Mechanisms of nickel-catalyzed coupling reactions and appplications in alkene functionalization," Acc. Chem. Res. **53**, 906 (2002).
[110]L. A. Burns, M. S. Marshall, and C. D. Sherrill, "Comparing counterpoise-corrected, uncorrected, and averaged binding energies for benchmarking noncovalent interactions," J. Chem. Theory Comput. **10**, 49 (2014).
[111]R. S. Grev and H. F. Schaefer III, "6-311G is not of valence triple-zeta quality," J. Chem. Phys. **91**, 7305 (1989).
[112]M. Reiners, A. C. Fecker, D. Baabe, M. Freytag, P. G. Jones, and M. D. Walter, "Cobalt and nickel compounds with pentadienyl and edge-bridged pentadienyl ligands: Revisited," Organometallics **38**, 4329 (2019).
[113]R. Jain, A. A. Mamun, R. M. Buchanan, P. M. Kozlowski, and C. A. Grapperhaus, "Ligand-assisted metal-centered electrocatalytic hydrogen evolution upon reduction of a bis(thiosemicarbazonato)Ni(II) complex," Inorg. Chem. **57**, 13486 (2018).
[114]R. Mondol and E. Otten, "Aluminum complexes with redox-active formazanate ligand: Synthesis, characterization, and reduction chemistry," Inorg. Chem. **58**, 6344 (2019).
[115]F. Neese, F. Wennmohs, A. Hansen, and U. Becker, "Efficient, approximate and parallel Hartree–Fock and hybrid DFT calculations. A 'chain-of-spheres' algorithm for the Hartree–Fock exchange," Chem. Phys. **356**, 98 (2009).
[116]A. Brakestad, P. Wind, S. R. Jensen, L. Frediani, and K. H. Hopmann, "Replication data for: Multiwavelets applied to metal-ligand interactions: Energies free from basis set errors," DataverseNO (2021).